Electronic Supplementary Material (ESI) for Physical Chemistry Chemical Physics.

Ion-ion interactions enhance aluminum solubility in alkaline suspensions of nano-gibbsite (α-Al(OH)$_3$) with sodium nitrite/nitrate

Mateusz Dembowski[†], Michelle M. Snyder[†], Calvin H. Delegard[‡], Jacob G. Reynolds[§], Trent R. Graham[†], Hsiu-Wen Wang[¤], Ian I. Leavy[†], Steven R. Baum[†], Odeta Qafoku[†], Matthew S. Fountain[†], Kevin M. Rosso[†], Sue B. Clark[†], and Carolyn I. Pearce[†]

[†]Pacific Northwest National Laboratory, Richland, Washington 99352, United States
[‡]Trade Wind Services, LLC, Richland, Washington 99352, United States
[§]Washington River Protection Solutions, LLC, Richland, Washington 99352, United States
[¤]Oak Ridge National Laboratory, Oak Ridge, Tennessee 37831, United States

TOC

Characterization

Magic angle spinning nuclear magnetic resonance (MAS-NMR)

^{27}Al MAS direct polarization (DP) experiments were conducted on a Bruker Ascend 600 MHz NMR spectrometer equipped with MASDVT600W2 BL2.5 X/Y/H probe. Samples were prepared by loading 2.5 mm commercial Bruker MAS rotors with as synthesized α-$Al(OH)_3$. ^{27}Al MAS-NMR spectra were collected using 0.450 µs pulse width, 18 ms acquisition time, and 2048 transients. MAS-NMR spectra were analyzed using Bruker TopSpin 4.0.5 software with 10 Hz line broadening. ^{27}Al chemical shifts are reported with respect to 1M $Al(NO_3)_3$ (H_2O, $\delta = 0$ ppm).

High-field ^{27}Al nuclear magnetic resonance (NMR)

^{27}Al NMR experiments were conducted on a Varian-Inova 750 MHz NMR spectrometer equipped with a 5-mm BBO probe operated at 25°C. Spectra were collected on samples contained in 4 mm Teflon inserts with the reference solution (1 M $Al(NO_3)_3$, H_2O, $\delta = 0$ ppm) so that both solutions were physically separated. One-dimensional ^{27}Al NMR spectra were collected using 56 dB power level attenuation, 19.5 ms pulse length, 1 s relaxation delay, and 1024 scans.

Inductively Coupled Plasma Optical Emission Spectrometry (ICP-OES)

Aluminum concentrations were determined using a PerkinElmer Optima 8300 dual view inductively coupled plasma optical emission spectrometer and a PerkinElmer S-10 auto-sampler interface at a wavelengths of 396.153 nm (axial). Calibration curves were generated using standards in the range from 50 ppb to 50 ppm (High-Purity Standards Corporation). This calibration was verified with an initial calibration verification (ICV) and continuing calibration verification (CCV), which was run every ten samples at a minimum. Continuing calibration blanks (CCB) were also analyzed after each calibration verification to ensure background signals and potential carryover effects were not a factor.

Ion Chromatography (IC)

Nitrite (NO_2^-) and nitrate (NO_3^-) concentrations were determined by either a Dionex Reagent Free Ion Chromatography System 5000 (RFICS-5000) with an AS-AP auto-sampler or a Dionex Reagent Free Ion Chromatography System 2000 (RFICS-2000) with an AS-1 auto-sampler. Calibration of both instruments was performed using a multi-component anion solution (Inorganic Ventures) in the range from 0.1 ppm to 7.5 ppm. This calibration was verified with an ICV and CCV standard run every ten samples at a minimum. A CCB (multi-component anion solution, SPEX CertiPrep) was analyzed after each CCV to ensure background signals and potential carryover effects were not a factor.

Total alkalinity

Alkalinity of the final solutions was measured using a Metrohm 888 Titrando Titrator controlled by a personal computer running Tiamo 2.4 software, with 0.02 N sulfuric acid (H_2SO_4) to a phenolphthalein endpoint for total alkalinity (hydroxide plus aluminate).

Brunauer-Emmett-Teller (BET)

The specific surface area of the α-$Al(OH)_3$ product was measured with an Accelerated Surface Area and Porosity System ASAP 2020, from Micromeritics. The sample was degassed at 75°C for nine hours, with a temperature ramp of 5°C/min. A Si-Alumina standard (Micromeritics) with a known surface area of 214 ± 6 m^2/g was analyzed immediately after the sample. The measured surface area of the standard was 212 m^2/g, which is within the accepted standard deviation range for the instrument.

Raman Spectroscopy

Raman spectra, in the 500-900 cm^{-1} spectral region was collected using Horiba LabRam HR spectrometer utilizing a Nikon Ti-E inverted microscope, 633 nm continuous light source, and 40x optical objective. Each spectrum is an average of ten, 60 second exposure times. The wavelength resolution and peak position uncertainty is ca. 1.2 cm-1 and 0.06 cm-1, respectively. A linear background correction was applied to all spectra using IgorPro 8 software package.

^{27}Al MAS-NMR of the α-$Al(OH)_3$ starting material

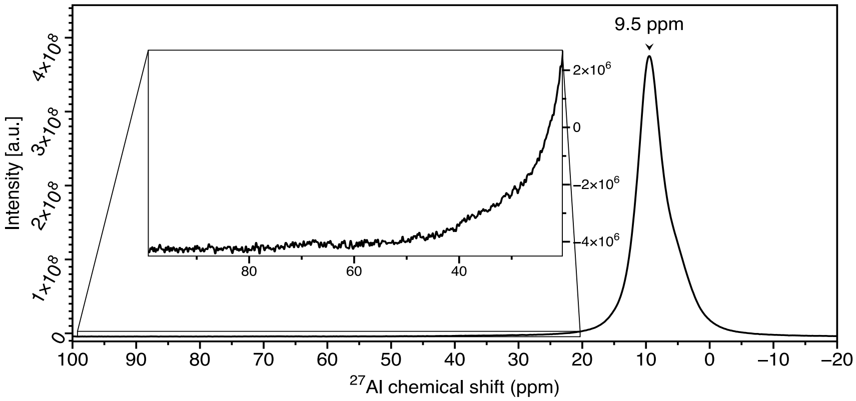

Figure S1. ^{27}Al MAS-NMR spectrum of α-$Al(OH)_3$ stock used in the current study. Inset to the left of the peak at ca. 9.5 ppm shows magnified spectral region from 30 to 90 ppm where penta- (40 ppm) and tetra-coordinated (80 ppm) Al species are expected to be observed. Spin rate = 20 kHz.

PXRD of the solid phases at the end of experiments

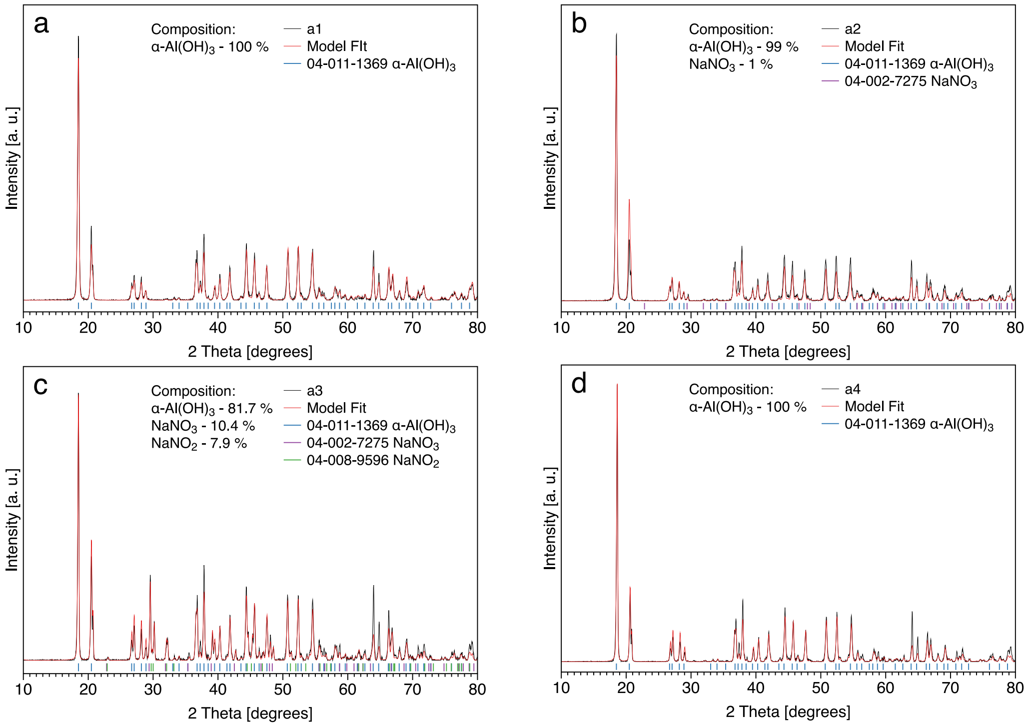

Figure S2. PXRD of solid phases extracted at the end of the experiments conducted at 45°C from undersaturation.

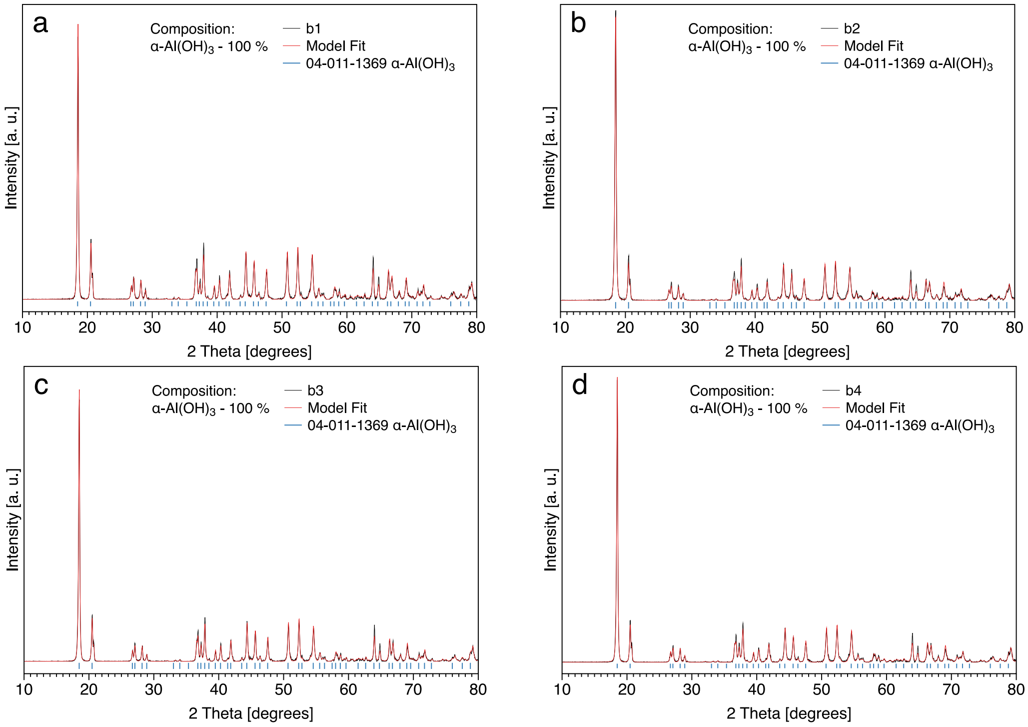

Figure S3. PXRD of solid phases extracted at the end of the experiments conducted at 45°C from oversaturation.

Pitzer model and literature solubility data

PHREEQC input data block

```
        DATABASE pitzer.dat      # must use DATABASE pitzer.dat
        TITLE Pitzer activity coefficients etc.

        SOLUTION_MASTER_SPECIES
        Al              Al+3                0           Al                  26.9815
        Al(+3)          Al+3                0           Al

        SOLUTION_SPECIES
        Al+3 = Al+3
                -dw        0.559e-9
                -Vm        -2.28  -17.1  10.9  -2.07  2.87  9  0  0  5.5e-3  1
        Al+3 + 4 H2O = Al(OH)4- + 4 H+
                -log_k     -22.7
                -delta_h 42.30      kcal
                -analytic  51.578    0.0        -11168.9  -14.865
        Al+3 + H2O = AlOH+2 + H+
                -log_k     -5.0
                -delta_h 11.49      kcal
                -analytic  -38.253   0.0        -656.27    14.327
                -Vm        -1.46  -11.4  10.2  -2.31  1.67  5.4  0  0  0  1
        Al+3 + 2 H2O = Al(OH)2+ + 2 H+
                -log_k     -10.1
                -delta_h 26.90      kcal
                -analytic  88.50     0.0        -9391.6    -27.121
        Al+3 + 3 H2O = Al(OH)3 + 3 H+
                -log_k     -16.9
                -delta_h 39.89      kcal
                -analytic  226.374   0.0        -18247.8  -73.597

        PHASES
        Gibbsite
                Al(OH)3 + OH-  = Al(OH)4-
                -delta_h  22.5 kJ  # Benezeth_2016
                -analytic  -96.5506   -0.0139828   2374.88   37.023242684  # Benezeth_2016

        PITZER
        #some parameters were regressed using a set of other parameters and therefore
        #may be dependent on these specific values of other parameters to reproduce data
        -macinnes   false
        -redox      false
        -B0
        Na+  OH-   0.0869   -356.02   -1.0814                                      # Pitzer_1991 in Weber_2001
#       Na+  OH-   0.091763   7118.75   45.78472   −0.07308                        # Reynolds_2015
#       Na+  OH-   0.0883443913   -1197.84571   -6.10983033   0.00743325156     # Xiong_2014
        Na+  Al(OH)4-   0.0513   -356.02   -1.0814                                 # Wesolowski_1992 in Weber_2001
        -B1
        Na+  OH-   0.2481    173.16   1.2073                                       # Pitzer_1991 in Weber_2001
#       Na+  OH-   0.212694   -46598   -279.171   0.414149                         # Reynolds et al. 2015
#       Na+  OH-   0.244421177    1627.02502   9.48250496   -0.0115788697          # Xiong_2014
        Na+  Al(OH)4-   0.2481    173.16   1.2073                                  # Wesolowski_1992 in Weber_2001
        -C0
        Na+  OH-   0.0039    34.22    0.0842                              # Pitzer_1991 in Weber_2001
#       Na+  OH-   0.001748   -267.9999   −1.7259   0.002725                       # Reynolds et al. 2015
```

```
#      Na+  OH-   0.00399943679   88.2475511   0.406876285  -0.000475666912 # Xiong_2014
       Na+  Al(OH)4-   0.0013    34.22    0.0842                        # Wesolowski_1992 in Weber_2001
       -THETA
       Al(OH)4-          OH-   0.014                                    # Wesolowski_1992 (also in Weber_2001 &
       Benezeth_2016)
       -PSI
       Na+                  OH-          Al(OH)4-   -0.0048             # Wesolowski_1992 in Weber_2001

####
Title Experiment Entries
SOLUTION 1 water
              pH    7.0 charge
              temp  25.0
              units mol/Kgw
              -water 1.0   #kg
Save Solution 1
END
EQUILIBRIUM_PHASES 1
      Gibbsite      0.0   0.0
USE Solution 1
USE equilibrium phases 1
REACTION_TEMPERATURE
   45
REACTION 1
              NaOH 1
              Al(OH)3 1
              20 moles in 40 steps
Save Solution 2
END
#
```

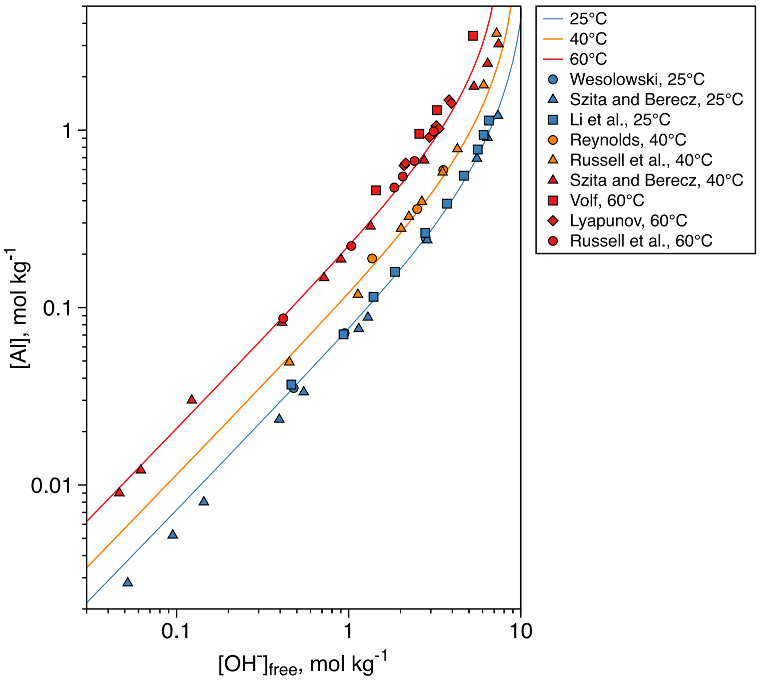

Figure S4. Comparison of the current α-Al$(OH)_3$ solubility model in α-Al$(OH)_3$-NaOH-H_2O system at 25°C (blue trace), 45°C (orange trace), and 60°C (red trace) with literature values.

27°C solubility experiments

Attainment of equilibrium from undersaturation at 27°C

Inductively coupled plasma optical emission spectrometry (ICP-OES) results from undersaturation (i.e. determined by dissolution of excess solid α-Al$(OH)_3$) are summarized in **Figure S5**. 27°C data demonstrates rapid dissolution and equilibration as indicated by the initial concentration measurements at three- and seven-days trending upward, but not exceeding the plateau concentrations ultimately attained at 76 days ($c1^{NO_2}$, $c2^{NO_3}$, and $c3^{NO_2/NO_3}$). The sinusoidal nature of Al concentration curves observed at 27°C is noteworthy with the lowest Al concentration at 21 days being about 80-85% of the final steady-state values. A plot of the data versus the temperature within the glovebox for these nominally 27°C tests (**Figure S6**) indicate that the Al concentrations fluctuate in accordance with changes in temperature. Thus, the temperature effect likely explains the variability. For the 27°C tests run in a pure OH^- system (c4), an initial rise but no apparent dip in concentration was observed. Rather, after attaining the maximum concentration value at seven days, steady-state concentration was reached. This anomalous behavior of the c4 samples with respect to $c1^{NO_2}$, $c2^{NO_3}$, and $c3^{NO_2/NO_3}$ is likely related to its propensity to sustain the metastable, supersaturated state more efficiently owing to its higher OH^- content.

Table S1. Mass based composition of stock solutions and the average mass of α-Al(OH)$_3$ used in triplicate experiments at 27°C (per 13 mL of stock solution)

Exp.	NaOH (g)	NaNO$_2$ (g)	NaNO$_3$ (g)	H$_2$O (g)	Al(OH)$_3$ (g)	Temp. (°C)
c1	4.094	48.432	0	99.581	0.204	27
c2	4.107	0	41.665	99.845	0.200	27
c3	4.060	34.329	46.322	99.887	0.200	27
c4	24.188	0	0	99.619	1.498	27

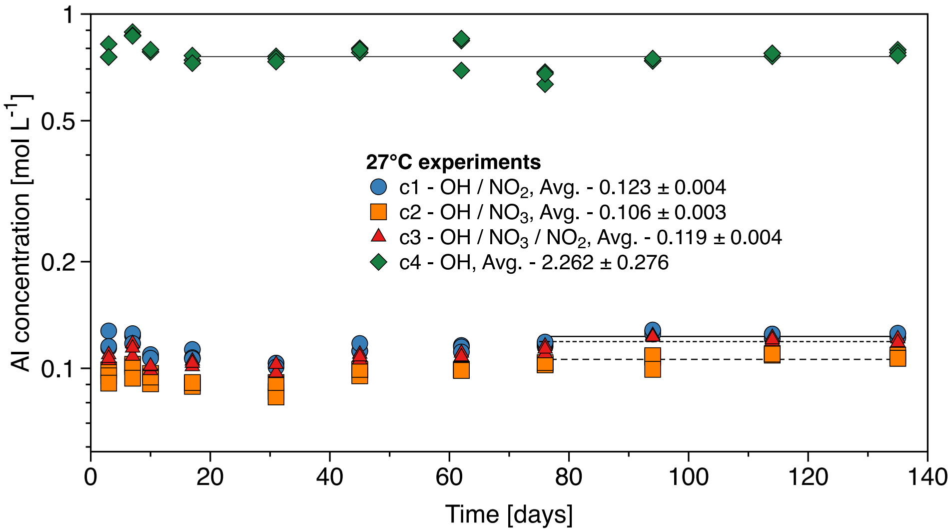

Figure S5. α-Al(OH)$_3$ solubility at 27°C as a function of varying NaNO2, NaNO3, and NaOH concentration. Horizontal lines indicate data regions used to obtain the displayed average plateau Al concentration.

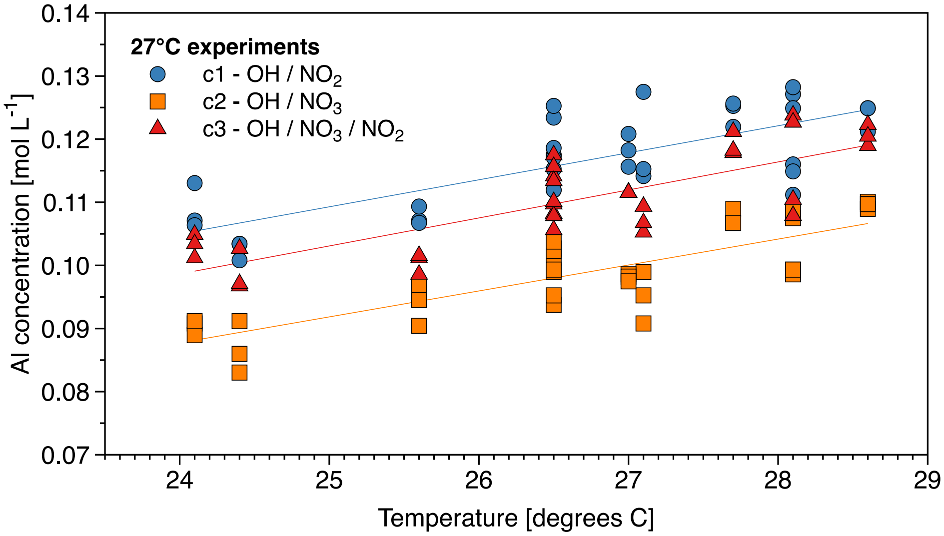

Figure S6. Dependence of α-Al(OH)$_3$ solubility on temperature in experiments c1-3.

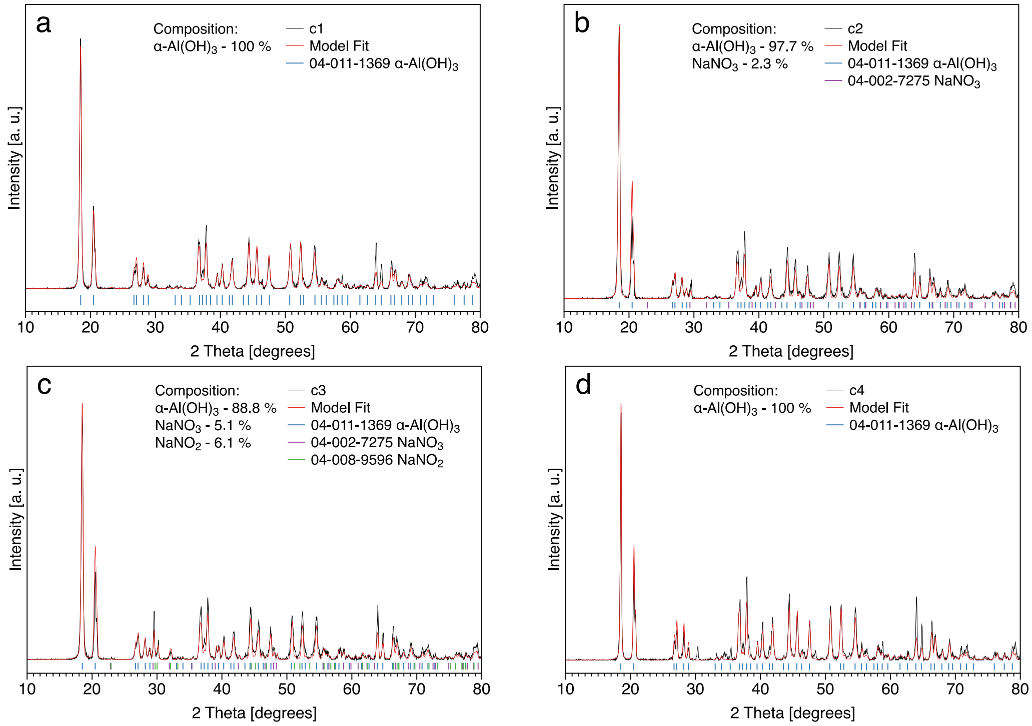

Figure S7. PXRD of solid phases extracted at the end of the experiments conducted at 27°C from undersaturation.

Table S2. Average solution temperatures, densities, solute concentrations (in mol kg^{-1}), predicted Al concentrations, $[Al]_{pred}$, and enhancement factors, Al_{enhc} at the final sampling

Exp.	$[OH^-]_{free}$ (m)	[Al] (m)	$[NO_2^-]$ (m)	$[NO_3^-]$ (m)	Density (g/cm^3)	$[Al]_{pred}$ (m)	Al_{enhc}[a]	Temp (°C)
c1	0.687	0.140	7.429	0	1.315	0.055	2.56	27.0
c2	0.759	0.109	0	4.662	1.295	0.061	1.80	27.0
c3	0.699	0.146	5.182	5.257	1.415	0.056	2.61	27.0
c4	4.838	0.691	0	0	1.275	0.583	1.19	27.0

[a] $Al_{enhc}=[Al]_{meas}/[Al]_{pred}$ where $[Al]_{pred}$ correspond to the Pitzer predicted [Al] concentration at observed $[OH]_{free}$.

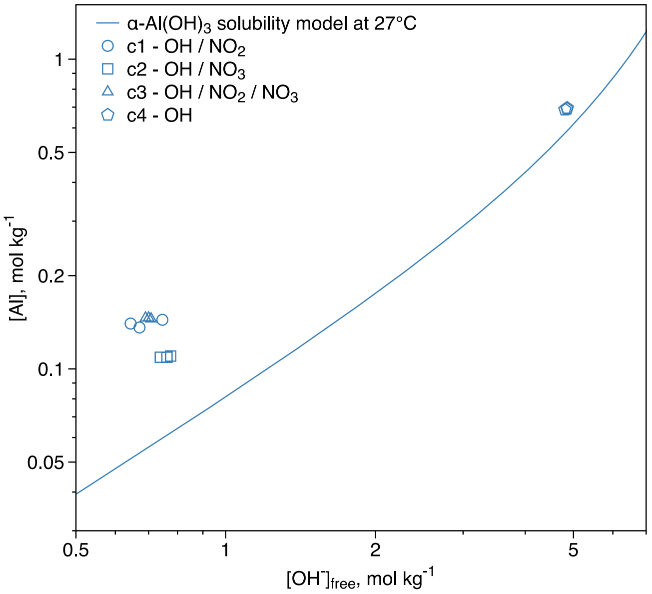

Figure S8. Measured α-Al$(OH)_3$ solubility in current experiments at versus solubility predicted from Pitzer model in the system of α-Al$(OH)_3$-NaOH-H_2O.

References:

(1) Pitzer, Kenneth S. *Activity coefficients in electrolyte solutions (2nd ed.).* Boca Raton: CRC Press. ISBN 0849354153 **1991**

(2) Weber, C. *Thermodynamic modeling of Savannah River evaporators*; Oak Ridge National Lab., TN (US): 2001.

(3) Reynolds, J. G.; Carter, R.; Felmy, A. R. A Pitzer Interaction Model for the $NaNO_3$–$NaNO_2$–NaOH–H_2O System from 0 to 100°C. *Ind. Eng. Chem. Res* **2015**, *54*, 3062-3070.

(4) Xiong, Y. A Pitzer Model for the Na–$Al(OH)_4$–Cl–OH System and Solubility of Boehmite (AlOOH) to High Ionic Strength and to 250° C. *Chem*. *Geol*. **2014**, *373*, 37-49

(5) Wesolowski, D. J. Aluminum Speciation and Equilibria in Aqueous Solution: I. The Solubility of Gibbsite in the System Na-K-Cl-OH-$Al(OH)_4$ from 0 to 100°C. *Geochim. Cosmochim. Acta* **1992**, *56*, 1065-1091

(6) Bénézeth, P.; Hilic, S.; Palmer, D. A. The Solubilities of Gibbsite and Bayerite Below 100° C in Near Neutral to Basic Solutions. *J. Solution Chem.* **2016**, *45*, 1288-1302.

(7) Berecz, E.; Szita, L., Electrochemical Method for Solubility and Dissolution of Solid Compounds - Some Thermodynamic Properties of System $Al(OH)_3$-NaOH-H_2O. *Electrochim Acta* **1970,** *15*, 1407.

(8) Li, H.; Addai-Mensah, J.; Thomas, J. C.; Gerson, A. R., *J. Colloid Interface Sci*, **2005**, *286*, 511-519.

(9) Russell, A. S.; Edwards, J. D.; Taylor, C. S., *JOM*, **1955**, 1123-1124

(10) Volf, F. F.; Kuznetsov, S. I., Polytherms in the Al_2O_3-Na_2O-H_2O System. *Zhurnal Pikladnoi Khimii (Zh. Prikl. Khim.)* **1955,** *28*, 597.

(11) Lyapunov, A. N.; Khodakova, A. G.; Galkina, Z. G., Solubility of Hydrargillite in NaOH Solutions Containing Soda or Sodium Chloride, at 60°C and 95°C, *Tsvetnyye Metally* [English Translation], **1964**, *37*, 48-51